



Analysis of electric loop in 1000KV UHV substation on anti-seismic and wind-resistance performance

S. Lin⁽¹⁾, P. Gao⁽²⁾, Z.C. Lu⁽³⁾, Z.L. Liu⁽⁴⁾, Y.H. Sun⁽⁵⁾

⁽¹⁾ Beijing, China, China Electric Power Research Institute, linsen@epri.sgcc.com.cn

⁽²⁾ Beijing, China, China Electric Power Research Institute, gaopo@epri.sgcc.com.cn

⁽³⁾ Beijing, China, China Electric Power Research Institute, luzc@epri.sgcc.com.cn

⁽⁴⁾ Beijing, China, China Electric Power Research Institute, liuzhenlin@epri.sgcc.com.cn

⁽⁵⁾ Beijing, China, China Electric Power Research Institute, sunyuhan@epri.sgcc.com.cn

Abstract

A numerical model of electric loop in 1000 kV UHV substation has been developed. The mechanical property of electric loop has been studied under earthquake excitation with peak amplitude of 0.2g (g is the acceleration of gravity) and 31.2 m/s strong wind condition. The max stresses of components have been obtained for different loading combinations. The results show that the max stress of electric equipment occurs near the base. Additionally, the safety margin can meet the requirements of relevant codes. The finite element analysis indicates that porcelain bushings have significant difference in dynamic responses. In order to optimize stress distribution of the electric equipment, suggestion on section design of porcelain bushing has been made in this paper.

Keywords: Ultra high voltage; Substation; Loop; Anti-seismic performance; Wind-resistance performance



1. Introduction

The electrical power system is an important component of lifeline project. Once destroyed in earthquake, it will be disastrous to social stability and economic development [1]. Because the substation equipment is generally composed of brittle porcelain or composite bushing, the interaction between the equipment through bus makes the seismic fragility pretty high [2]. In Wenchuan earthquake, substation equipments were suffered a severe damage. However, only 500 kV and below electrical equipments locate there [3]. For 1000 kV substation equipments, they are bigger, higher, more heavy, more flexible, easier to destroy. Therefore, anti-seismic and wind resistant performance check of the electrical equipment in the loop should be focused on. In addition, component optimization under certain load is helpful, which makes mechanical equilibrium.

The anti-seismic and wind resistant performance analysis on loop in 1000KV ultra high voltage (UHV) substation has been accomplished in this paper. The max stress and top displacement of the electrical equipment and the internal force of fitting have been obtained under wind and seismic load somewhere for the 100-year return period. Components in the loop have been optimized to improve the reliability when suffered external loads. More importantly, the weak link in seism has been strengthened.

2. Modeling of UHV loop

2.1 Introduction of UHV loop

The UHV loop consists of gas insulated switchgear (GIS), arrester, transformer, high voltage shunt reactor. The GIS and tube bus are connected by flexible conductor. The arrester and transformer are connected to tube bus by slipping fitting and support clamp respectively. The high voltage shunt reactor and tube bus are connected by soft link fitting. The transmission force of flexible connection can be ignored. Therefore, the only system that needs to be calculated is the loop comprising arrester and transformer, which are connected by tube bus. The height of the loop is 18 m. The distance between arrester and transformer is 8.5 m. Casings of arrester and transformer are made up by high tension porcelain. Electrical equipment stents are composed of steel pipes with specifications for $\phi 194 \times 12$ and $\phi 83 \times 8$. The tube bus is composed of aluminum pipe with specification for $\phi 200 \times 10$. The sectional drawing of the loop and unfolded drawing of stents are shown in Fig. 1 and Fig. 2. The material property parameters of each component in loop are listed in table 1.

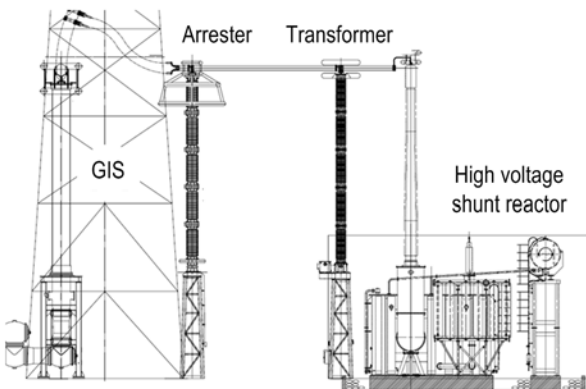


Fig. 1 – Sectional drawing of loop

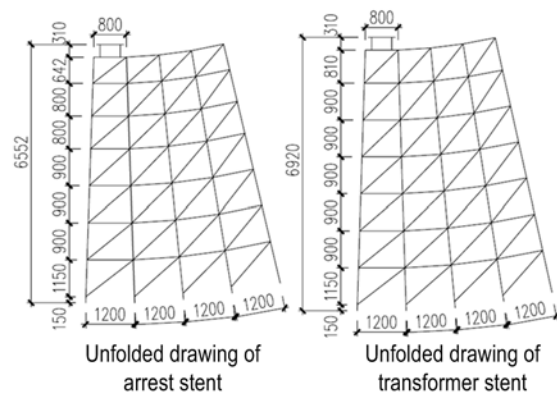


Fig. 2 – Unfolded drawing of stent



Table 1 – The material property parameters of each component in loop

Component	Material	Density (kg.m ⁻³)	Elastic modulus (N.mm ⁻²)	Poisson ratio	Failure stress (MPa)
Arrester	High tension porcelain	2700	9×10 ¹⁰	0.3	55
Transformer			1.1×10 ¹¹	0.3	55
Stent	Q235 steel	7850	2.06×10 ¹¹	0.3	—
Tube bus	Aluminum	3105	7×10 ¹⁰	0.3	—

2.2 Numerical model of the loop

The three-dimensional finite element model has been established using software ANSYS. The axial direction of tube bus is defined as X direction of the model. The stents under the loop are rigid connected with ground, and the interaction between foundation and loop is not considered in this paper. Based on the mechanics feature of each component in the loop, proper element types are applied to simulating corresponding structures. The arrester, transformer and tube bus are simulated with beam elements. The stent is simulated with link and shell elements.

The material properties of porcelain bushings are listed in table 1, which are test results provided by equipment manufacturer. The physical property parameters of porcelain bushings are shown in table 2.

Table 2 – The physical property parameters of porcelain bushings

Components	Weight (kg)	Length (m)	Outer diameter (m)	Inner diameter (m)	Frontal area (m ²)
Arrester bushing	742	2.12	0.51	0.40	1.88
Transformer bushing	694	2.17	0.44	0.34	1.65

The electrical equipment flange is simulated with an equivalent beam element, whose sectional moment of inertia and bending rigidity are determined. The sectional moment of inertia can be formulated as follows [4]:

$$I_c = K_c \frac{L_c}{E_c} \quad (1)$$

where I_c is the inertia moment of the section, L_c is the length of beam element, E_c is the elastic modulus of porcelain bushing. The bending rigidity K_c can be written as follows:

$$K_c = 6.54 \times 10^7 \frac{d_c h_c}{t_c} \quad (2)$$

where K_c is the bending rigidity, d_c is the cementing part diameter of porcelain bushing, h_c is the cementing height, t_c is the cementing height clearance.

The finite element model of loop is shown in Fig. 3, which contains 1895 elements and 2142 nodes.

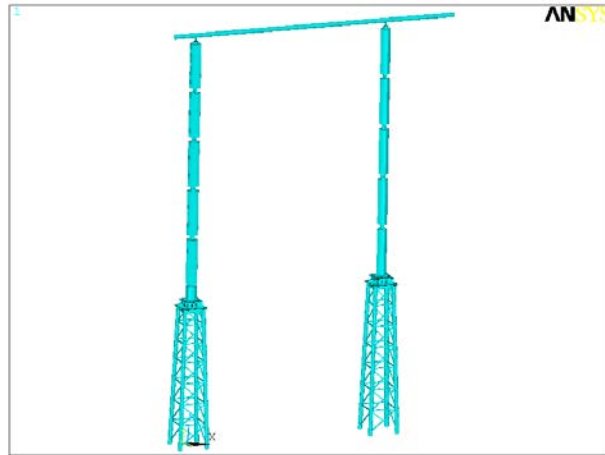


Fig. 3 – Finite element model of loop

3. Input load

On the basis of reference [5] and reference [6], the wind load can be calculated as shown in table 3. The basic wind pressure of 100-year return period is considered, namely wind velocity 31.2 m/s. The value of each coefficient depends on the shape feature of the component. The wind load is the product of the wind load standard value and the frontal area.

Table 3 – Wind load of the structure

Position	Wind load (kN)	
	Arrester	Transformer
The first porcelain bushing	6.15	3.50
The second porcelain bushing	2.61	1.51
The third porcelain bushing	2.47	1.42
The fourth porcelain bushing	2.33	1.35
The fifth porcelain bushing	2.33	1.35
Stent	7.34	7.91
Tube bus	2.19	

The artificial earthquake wave excitation with peak amplitude of 0.2g is adopted for the seismic performance evaluation. According to reference [4], parameters of seismic action, which are necessary for constructing the earthquake acceleration response spectra, can be determined as shown in table 4. The damping ratio of electrical equipment in the loop adopts recommended value 2% in IEEE for seismic design of substations. The generated horizontal response spectra is shown in Fig. 4.

Table 4 – Relevant parameters of seismic action

Characteristic period (s)	Site classification	The max horizontal seismic coefficient
0.45	II	0.57

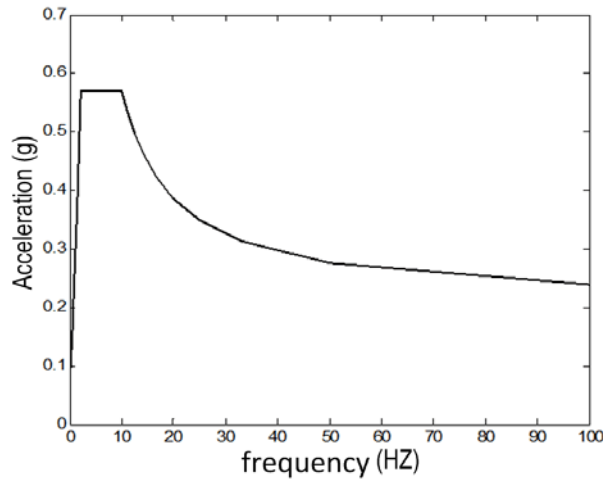


Fig. 4 – Horizontal response spectra

The combinatorial load should be considered in the analysis [7]. Combinatorial patterns of loads for various conditions are shown in table 5.

Table 5 – Combinatorial patterns of loads

Condition	Combinatorial pattern of loads
Strong wind	$S = S_{GE} + S_w$
Earthquake	$S = S_{GE} + 0.25S_w + S_E$

where S_{GE} represents gravity load, S_w is wind load, S_E is seismic load. When calculating the response of the electrical equipment under the wind load, wind load is input along Y direction, namely the control direction of wind resistant calculation. When it comes to seismic effect, the response is governed by seismic load. The response spectra is input in X direction and Y direction respectively, and the direction of wind load is the same.

4. Analysis method

Analysis of wind condition is static analysis. Gravity load and wind load are uniformly distributed on each component. The response of the component under the wind load can be obtained after solving.

For mechanical performance analysis under seismic action, static analysis is carried out at first. Then dynamic analysis should be achieved. Block Lanczos method is applied to the modal analysis. The seismic response of the loop can be computed by the mode superposition method. Finally, the response of the loop under seismic action condition can be obtained by combining results of static analysis and dynamic analysis.

5. Result and discussion

5.1 Result of modal analysis

Through mode analysis on loop system, natural frequencies and vibration modes which can reflect structural dynamic characteristics are obtained. Meanwhile, the modal participating factor and the effective mass of the structure in each direction is calculated. The modal participating factor which is a function of the vibration mode and the excitation orientation can indicate the modal energy contribution. The effective mass participation also reflect vibration participation level of the structure for the frequency. For sufficiently accurate results, The first

100 order modes are adopted in calculation, and the effective mass accounted for more than 90% of the overall structure.

The first two natural frequencies of the loop are 1.19 Hz and 1.25 Hz. The vibration direction of the first order mode and the fourth order mode is direction X. Meanwhile the vibration direction of the second order mode and the third order mode is direction Y. The first 10 order frequencies are listed in table 6. Additionally, the structural vibration shape of the first 4 order vibration modes are shown in Fig. 6.

Table 6 – Analysis results of the first 10 order modes

Order	Frequency (Hz)	Effective mass participation			Effective mass (kg)		
		X	Y	Z	X	Y	Z
1	1.19	1.0000	0.0035	0.0004	4997.59	0.07	0.00
2	1.25	0.0047	1.0000	0.0000	0.11	6028.20	0.00
3	1.33	0.0033	0.6649	0.0001	0.06	2664.78	0.00
4	1.41	0.8646	0.0042	0.0004	3736.12	0.10	0.00
5	4.48	0.0237	0.0003	0.0516	2.81	0.00	22.21
6	4.56	0.0018	0.0813	0.0001	0.02	39.83	0.00
7	6.18	0.7057	0.0154	0.0029	2488.68	1.42	0.07
8	6.26	0.0143	0.5524	0.0001	1.03	1839.47	0.00
9	6.62	0.0229	0.7145	0.0001	2.62	3077.10	0.00
10	6.93	0.7093	0.0202	0.0008	2514.52	2.45	0.01

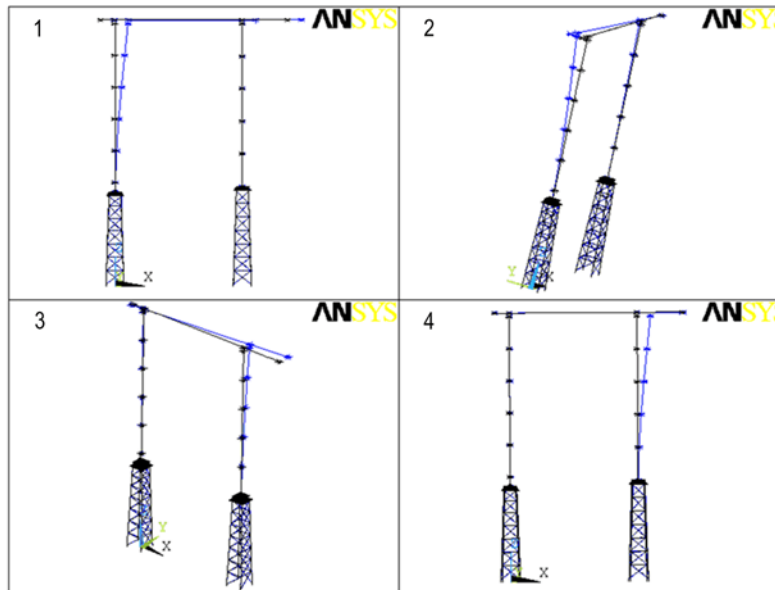


Fig. 5 – The first fourth order modes of loop

5.2 Result of anti-seismic and wind-resistance performance analysis

Responses such as the stress and displacement of the equipment, the fitting internal force are list in table 7. Under the seismic action and wind load, the max stress of the equipment appears on the root. However, the max stress of the sent appears on the top. The max stress of tube bus occurs at the junction with the equipment. The max displacement of loop happens on the tube bus when undergoing seismic action in Y direction.



Table 7 – Max stresses of the equipment

Position	Strong wind condition		Seismic action in X direction		Seismic action in Y direction	
	Arrest	Transformer	Arrest	Transformer	Arrest	Transformer
The first bushing	1.09	1.48	2.15	2.24	2.05	2.72
The second bushing	3.38	3.9	5.48	6.32	5.47	6.66
The third bushing	6.33	6.91	9.31	11.13	9.63	10.98
The fourth bushing	9.91	10.48	13.72	16.69	14.45	15.94
The fifth bushing	14.1	14.6	18.84	23.18	19.94	21.93
Stent	114.12	76.2	147.14	114.9	154.97	109.9
Tube bus	7.57		10.53		10.06	

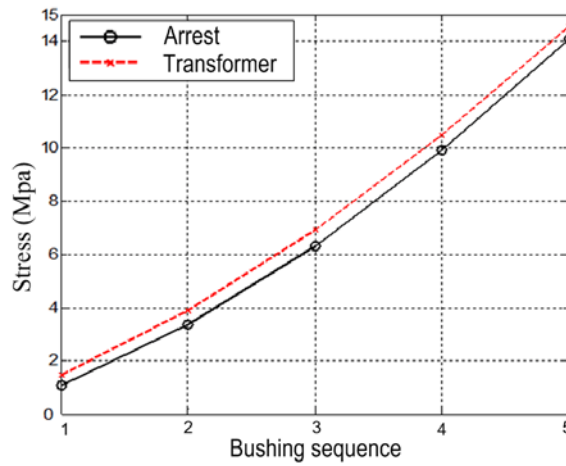


Fig. 6 – Max stresses under wind condition

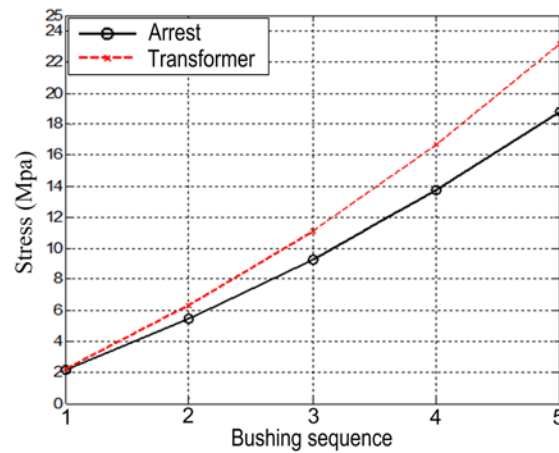


Fig. 7 – Max stresses under seismic action for X direction

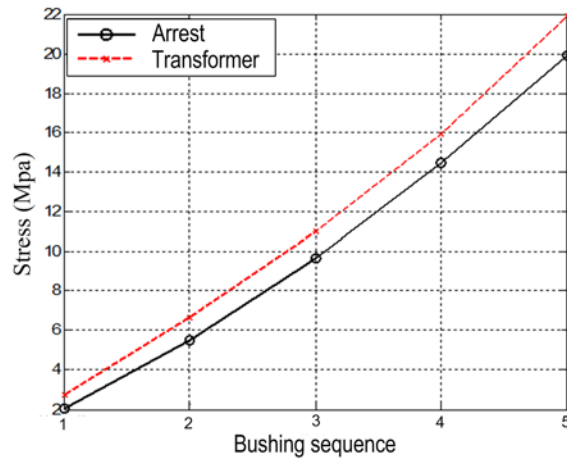


Fig. 8 – Max stresses under seismic action for Y direction

The max stresses of the equipment under wind condition and seismic action are shown in Fig. 6 ~ Fig. 8. The max displacements of the equipment under wind condition and seismic action are listed in table 8.

Table 8 – The fitting internal force and max equipment displacement

Condition	Fitting internal force (N)		Equipment displacement (mm)	
	Horizontal	Vertical	Arrest	Transform
Strong wind	1404.66	3055.71	69.96	51.56
Seismic action in X direction	3529.02	3371.38	95.82	81.73
Seismic action in Y direction	2943.3	3060.69	101.27	78.27

The stress nephogram and displacement nephogram are shown in Fig. 9 and Fig. 10.

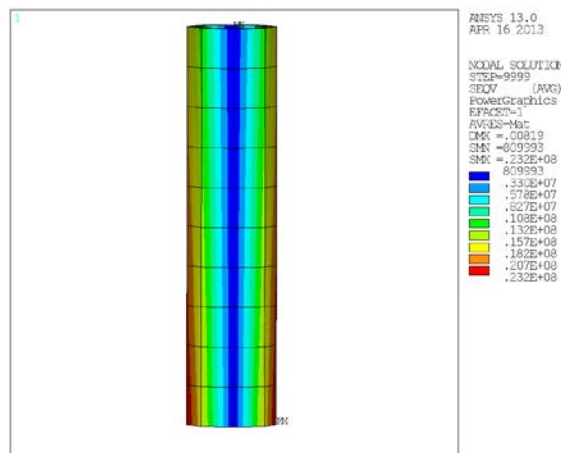


Fig. 9 – Stress nephogram of transformer bottom for seismic action in X direction

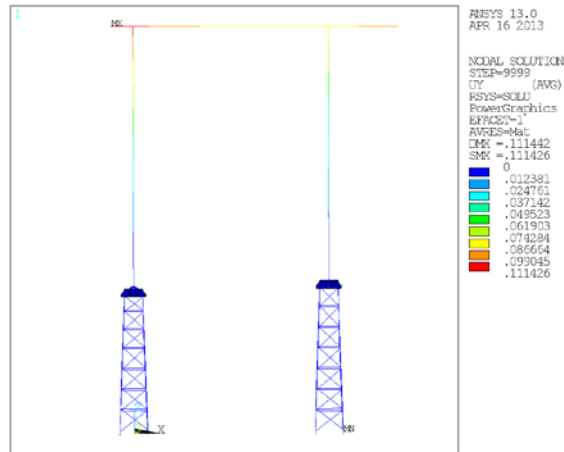


Fig. 10 – Loop displacement for seismic action in Y direction

Under the wind load, the max displacement of equipments is 69.96 mm. While that is 101.27 mm under seismic action. Under the wind load, the max stress of equipments is 14.6 Mpa. The failure strength of equipment is 55 Mpa, which is test result provided by equipment manufacturer. The overstrength is 3.77, namely the ratio of failure strength and the calculated stress. Those are 23.18 Mpa and 2.37 respectively under seismic action. The simulated safety margins are all meet the requirement.

From the view of the stress distribution of each section of the porcelain bushing, the maximum stresses of porcelain bushings vary greatly. For example, the stress of top bushing is only 2.24 Mpa and the stress of bottom bushing reaches 23.18 Mpa. To improve the stress distribution, Increasing cross-sectional area of the bottom bushing and decreasing that of the top bushing can be considered. The stress will distribute more balanced by making full use of the bearing capacity of each porcelain bushing.

6. Conclusion

The numerical model of the 1000KV UHV loop has been developed using software ANSYS. The mechanical property for strong wind with velocity 31.2 m/s and earthquake with peak amplitude of 0.2g have been studied. The results show that the max stresses of equipment are 14.6 Mpa and 23.18 Mpa for wind load condition and seismic action condition respectively, which can meet the requirement for electrical equipment safety. The great stress gap from the electrical equipment top to bottom indicates imbalance stress distribution. Appropriately adjusting the cross-sectional area of each porcelain bushing is proposed as an optimization suggestion.

7. Acknowledgements

The paper was supported by the scientific research program of "Seismic performance optimization technology research on pillar type electrical equipment and converter loop system of UHV converter substation" (GCB17201500063) from SGCC.

8. References

- [1] Guo ZY (2005): Research on performance of transformer against seism. *Transformer*, **42** (8S), 13-31.
- [2] Xie Q, Wang YF (2009): Seismic failure analysis on substation switch equipments in Wenchuan earthquake. *Journal of Shenyang Jianzhu University: Natural Science*, **25**, 1050-1057.
- [3] Zhang XH, Wu GN, Jiang W, Ren ZC, Peng Q (2009): Effects of Wenchuan earthquake on Sichuan grid. *Modern Electric Power*, **26** (4), 4-9.
- [4] Zhang XJ (2013): *GB 50260-2013 Code for seismic design of electrical installations*. China Planning Press, Beijing.
- [5] Huang SM (2010): *GB 50011-2010 Code for seismic design of buildings*. China Architecture & Building Press, Beijing.



- [6] Jin XY (2012): *GB 50009-2012 Load code for the design of building structures*, China Architecture & Building Press, Beijing.
- [7] Wu XF, Sun QG (2011): Seismic analysis of an UHV suspended converter valve tower. *World Earthquake Engineering*, 27 (2), 207-210.